Damage Detection with Ultrasonic Guided Waves Based on Broadband Random Excitation and Stochastic Signal Processing

Jonas Brettschneider[1(✉)], Peter Kraemer[1], Pawel Kudela[2], and Jochen Moll[3]

[1] Chair of Mechanics/Structural Health Monitoring, University of Siegen, Siegen, Germany
jonas.brettschneider@uni-siegen.de
[2] Institute of Fluid-Flow Machinery, Polish Academy of Sciences, Warsaw, Poland
[3] Institute of Physics, Goethe University of Frankfurt am Main, Frankfurt, Germany

Abstract. In the last decades, ultrasonic guided waves have proven to be a promising tool for structural health monitoring (SHM). For a number of reasons, narrowband burst signals are widely used to excite structures in order to reduce the impact of multimodal wave propagation and dispersion. This paper addresses a different approach using broadband random excitation signals. While burst signals are advantageous for damage localization and compensation of environmental and operational conditions, the interference of stochastic waves resulting in a complex wavefield could be more sensitive to structural changes, including defects. Based on promising experimental results published recently, potentials and limitations resulting from random excitation are investigated in this paper. Sensor signals are simulated using the time domain spectral element method for a carbon fiber composite plate and twelve piezoelectric transducers. The simulated sensor signals are analyzed using different statistical methods, including the Nullspace-based Fault Detection algorithm known from vibration-based SHM, to compute damage indices for the intact and damaged states of the plate. Moreover, wavefield images computed by the root mean square (RMS) are presented. Detected defects and non-visible damage positions are compared and the results are discussed.

Keywords: Structural Health Monitoring · Guided waves · Signal processing · Random excitation · Composites

1 Introduction

There are various upsides using narrowband bursts signal for guided waves based SHM. One of the main benefits is the reduced complexity of wave propagation. Regarding guided waves in general, multimodal wave propagation and dispersion lead to complex wavefields and measured signals that are difficult to interpret, especially under changing environmental conditions. Narrowband tone burst excitation can be used to simplify the

P. Rizzo and A. Milazzo (Eds.): EWSHM 2020, LNCE 127, pp. 788–797, 2021.
https://doi.org/10.1007/978-3-030-64594-6_76

resulting signals, especially when combined with wave tuning. Changes in the signals can then be identified in the simplest case by subtracting baseline signals from currently measured ones or by using additional signal processing [1].

A different approach using stochastic excitation or diffuse wavefields was used multiple times in vibration based SHM and was recently transferred to guided waves [2]. The reasons for this approach are related to possible advantages of the complex wavefields; due to the interfering nature they might be more sensitive to changes than narrowband tone bursts. This could lead to several benefits, either the detection of smaller damages or the application of less sensors. Another advantage could be the exploitation of ambient excitation so that potentially no active excitation would be required and therefore the weight of SHM-systems could be reduced.

In recent examples different ways of excitation were used to generate diffuse wavefields, one example is to use high pressured air that is randomly sprayed over the tested plate [3]. Another research group worked with a pulsed Nd:yttrium-aluminum-garnet-laser enabling local excitation at various positions [4]. The analysis in both cases was based on Greens function. The transfer function between sensors was calculated and compared in different structural conditions. Due to the path-based analysis at least weak localization of damage was possible.

The analysis in this paper is based on simulated data. This has on one hand several advantages, for example all unwanted influences, like temperature or humidity are excluded. In addition, different damage cases or sensor distributions can be tested without too much expenses later on. On the other hand, simulated data could be corrupted by different numerical errors and discrepancies between the model and reality. The simulated signals used for analysis later on are computed using the spectral elements method, known for excellent modeling of wave propagation [5].

The simulated model consists of a carbon fiber composite plate and twelve piezoelectric transducers. One transducer is always used in turn as an actuator while the others sense the simulated signals. Four different states of the model are simulated and the following methodology is used to identify damaged and undamaged states: The excitation signal for the actuator consists of white noise to generate a complex wavefield; the resulting signals at the sensors are then analyzed using different techniques especially by means of the Nullspace-based Fault Detection algorithm (NSFD). Damage is simulated in this model at different positions on the plate in form of delamination.

The novelty of this approach is to simulate and analyze data of diffuse wavefields generated by piezoelectric transducers with stochastic input signals. Because the approach is not based on path related damage indicators, localization will be rather difficult and the approach will need to be combined with additional algorithms.

2 Numerical Simulations

2.1 The Time-Domain Spectral Element Method

The time-domain spectral element method [5] was used for numerical simulations of propagating elastic waves. A flat shell element was used which is based on Mindlin-

Reissner first-order shear deformation theory. It has 36 nodes and 5 degrees of freedom at each node: displacement components along three axes and two independent rotations of cross-sections.

Parallel implementation, similar to the one presented in Ref. [6], was used to speed up computations. The proposed approach differs in the calculation of elemental forces which depend on the contribution of the extensional stiffness, the flexural stiffness, bending-stretching coupling, twisting-stretching along with bending-shearing coupling, stretching-shearing coupling and bending-twisting coupling instead of the matrix of elastic constants assigned to each layer of a composite laminate. Hence, the proposed method is more suitable for wave propagation modelling in multilayer composite laminates because it leads to a much lower number of degrees of freedom (see [7] for more details).

2.2 The Numerical Model

The structure under investigation was quasi-isotropic carbon-fibre-reinforced polymer (CFRP). The assumed layup of the composite was [45/0/-45/90/-45/0/-45/0/45/90]. The dimensions were 500 mm × 500 mm and the thickness 2 mm. The assumed material properties of unidirectional CFRP are given in Table 1. The assumed mass density was 1571 kg/m^3.

Table 1. Material properties of unidirectional CFRP (Units: GPa), see [8] for more details.

C_{11}	C_{12}	C_{22}	C_{44}	C_{55}	C_{66}
130	6.1	11.2	3.0	4.2	4.2

Piezoelectric transducers of the diameter 10 mm and the thickness 0.2 mm were taken into consideration in the model by changing local inertia and stiffness in corresponding spectral elements. The composite laminate was modelled by using one layer of spectral flat shell elements at its neutral plane. However, the contribution of all composite layers to the overall elemental stiffness was taken into account in the usual way.

Three locations of delamination of diameter 10 mm were investigated. The delamination locations and arrangement of 12 piezoelectric transducers is presented in Fig. 1. Each delamination case was considered separately. Two layers of flat shell spectral elements were used at delamination location in order to mimic separation of composite layers. Furthermore, contribution to the stiffness is divided into upper and lower elements according to the position of the delamination in between composite layers (it was assumed that the delamination is between 4th and 5th composite layer).

Other important parameters used in the numerical simulation are the total wave propagation time of 1.3 ms, the number of elements 9360 and number of nodes 234 612. It gives on average 1 mm spacing between nodes. It should be noted that the mesh is dense enough for wavelength up to about 5 mm. However, due to random excitation,

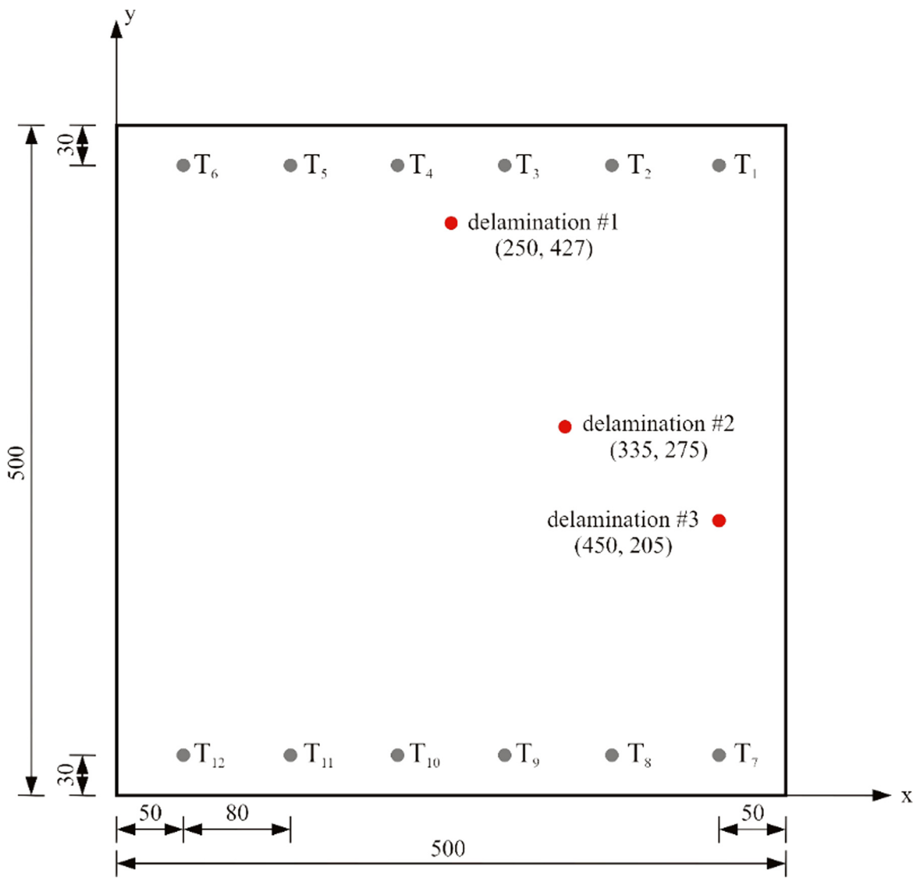

Fig. 1. The geometry of the analyzed composite laminate, see [8].

higher frequencies and shorter wavelengths are generated which are not properly modelled. But the conceptual work presented here is not affected by that. The mesh density was selected to achieve reasonable computation time. The time integration step equal to 0.0106 ms was chosen to assure the stability of the solution.

The random excitation was applied to the transducer T_1 and signal voltages were collected at all 12 transducers. Additionally, transverse displacements at the top surface were computed on a uniform grid of 500 $\times$ 500 points (for full wavefield analysis). The simulation was repeated 5 times to have 5 different random excitations and corresponding responses. Next, the simulation was repeated in the same manner for transducer T_2 and so on. The procedure was repeated 4 times which covers delamination locations #1, #2, #3 and reference state. The total number of simulations was 240.

3 Data Analysis

3.1 Full Wavefield Signal Processing

The aim of full wavefield analysis is verification whether the randomly excited propagating waves contain damage-related information. Each frame of propagating waves was processed by using a median filter with kernel size 3×3. Next, the frames were combined by using weighted root mean square (WRMS). Essentially WRMS gives information about the spatial distribution of energy.

The energy distribution is shown in Fig. 2. High values of the presented map can be seen at the excitation area and delamination area of corresponding delamination locations. Of course, for the reference case (Fig. 2d) high values occur only at transducer location. The energy distribution maps confirm that signals of propagating waves contain damage-related features. It is important to note that each delamination can be precisely localized although the excitation was stochastic.

3.2 Damage Detection Analyzing the Simulated Signals

Nullspace-Based Fault Detection Algorithm. The main tool to analyze the signals is the NSFD, known from vibrations based SHM. The algorithm is based on state-space models that are able to describe the behavior of the monitored structure. Using the covariance-driven approach the respective modelling is defined by system matrices derived from auto- and cross-correlation of measured signals in form of a Hankel matrix. Structural changes of the monitored structure result in changes in the respective Hankel matrix and can be detected using the nullspace of reference Hankel matrices. Further explanation regarding the algorithm can be found in various literature [9].
The vibration-based approach, of course, cannot be transferred one-to-one to guided wave-based SHM. In contrast to vibration-based structural monitoring, the NSFD cannot detect modal changes here. However, it is a promising mathematical tool to detect changes in wave fields as well. The two most important requirements are simultaneous recording of the signals and broadband stochastic excitation.

On the following pages a number of figures will be presented, illustrating different kinds of damage indices (DIs). All of them are organized in a similar form. The first measurement of the undamaged state is chosen to be the reference state and no DI will be displayed due to fixed values. First four DIs will refer to the undamaged state, while indicators 6-10 refer to delamination at position 1 (see Fig. 1), 11–15 refer to position 2 and 16–20 to position 3. In addition, the average value for each structural state will be presented on top of respective bars.

The following figure shows the DI_{NSFD} calculated using the NSFD for excitation at transducer six (T_6) as an example. In general, the results can change due to the position of the excitation, but in this study the differences in the results, especially for delamination at position 2 and 3, are rather small and excitation at position 6 is presented as representative for all the others. The delamination at position one, however, is a lot harder to be observed and its detection does depend on the actuator position. In this example signals of eleven sensors have been analyzed to calculate the DI_{NSFD} (Fig. 3).

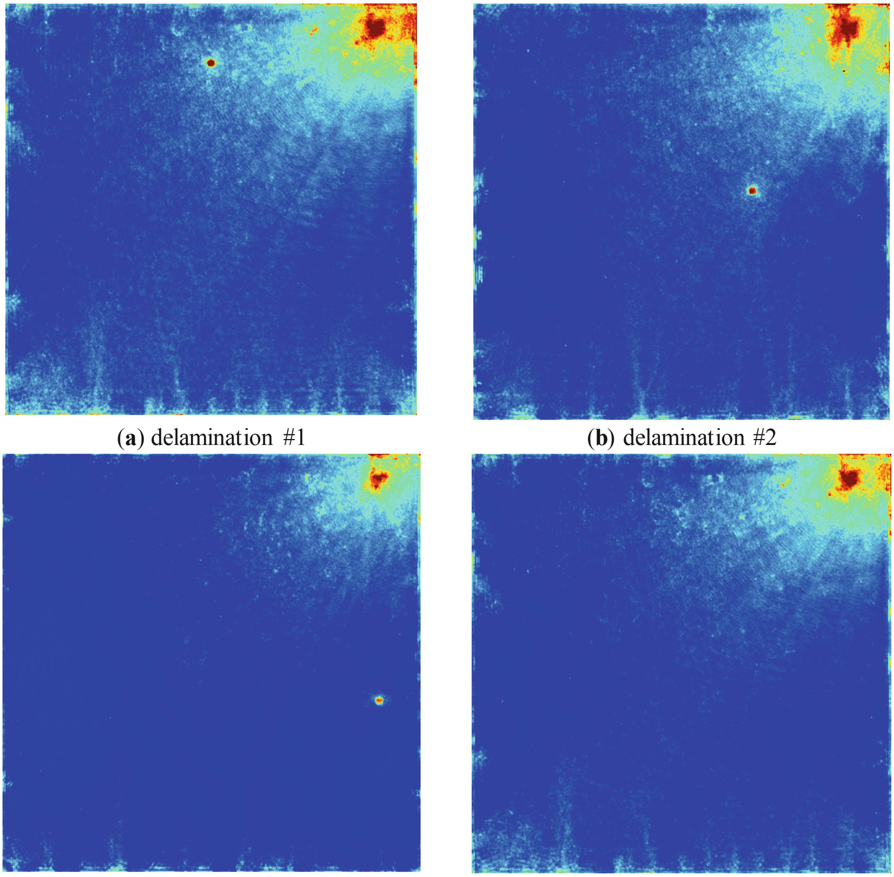

(**a**) delamination #1 (**b**) delamination #2

(**c**) delamination #3 (**d**) reference

Fig. 2. Wavefield energy for the case of excitation at transducer T_1.

The next example shows the DI_{NSFD} computed under same excitation conditions but using only the signals of T_{9}-$_{12}$. This sensor configuration was chosen, since in this case there are no delamination on the direct path between sensors and actuator. Also, in this case the changes in the global wavefield can be well detected (Fig. 4).

Again, delamination at position 2 and 3 are clearly detected while position 1 is barely visible. This leads to the observation that the influence on the wave field at this location is smaller than at the other positions and further investigation in the future might show why this is the case. In this paper, however, the focus will continue to be on the signal processing techniques that are able to detect the changes in signals due to delamination at different positions.

Damage Detection Based on Auto- and Cross Correlation Vectors. There is a certain disadvantage using NSFD; the time needed to compute DIs is increasing drastically using multiple sensors and an increasing number of timesteps for the

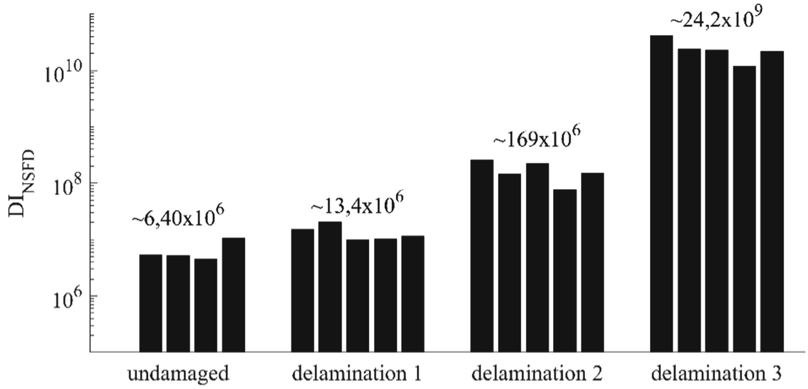

Fig. 3. Results of NSFD algorithm using all sensors; excitation at T_6.

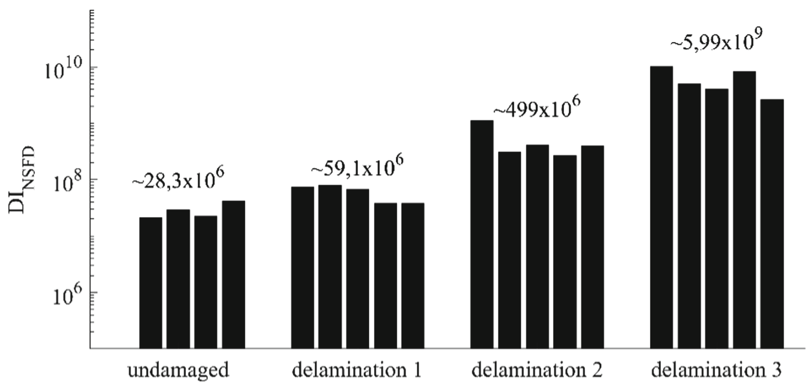

Fig. 4. Results of NSFD algorithm only using the sensors $T_{9\text{-}12}$.

computation of the Hankel-Matrix. To make live monitoring more easily another algorithm was derived demanding less computational time. Here, the vectors of the auto- and cross-correlation functions are computed in the same way as for NSFD. The length of the resulting vectors corresponds to the number of selected time shifts, while the number of vectors corresponds to the number of possible sensor combinations. Since there are 11 sensors 66 differing combinations of sensors are possible and 15360 time shifts have shown to deliver good results. The resulting 66×15360 matrix can be computed for every measurement and another DI can be calculated by comparing these matrices.

An easy way to do so is to calculate the correlation coefficient for corresponding columns and then average the 66 results to get the DI_{corr} shown in Fig. 5. Using the correlation coefficient of course means that the DI_{corr} should decrease if structural changes occur. The advantage is of this approach is decreased computation time because no singular value decomposition has to be calculated and accordingly more

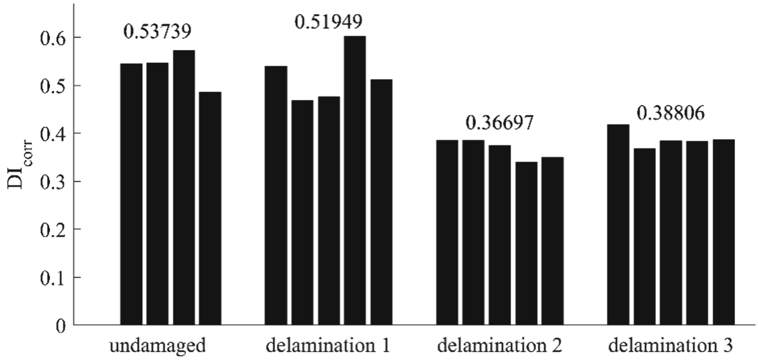

Fig. 5. Results using the algorithm based on correlation vectors; all sensors; excitation at T_6.

timesteps can be used and live monitoring would be easier. The downside is reduced sensitivity and clarity of DIs.

Further Signal Processing Based on Simple Spectra Analysis. The presented algorithms are designed to detect changes in the structural behavior and therefore in the resulting wavefield of the monitored object. Knowledge about the type of change is crucial for effective use of the algorithms. This part is focusing on further signal processing to investigate what type of change is detected in the signals. There are countless possibilities to analyze stochastic signals, but in this case frequency analysis delivers promising results.

The first step to compare the different states of the simulated plate was to compute the power spectral density for one signal in every simulated measurement. In this case the signal received at T_7 while excitation took place at T_6 was picked as an example. Knowing that measurements 1–5, 6–10, 11–15 and 16–20 belong to the 4 different states they were averaged to get four respective spectra to compare with each other (Fig. 6).

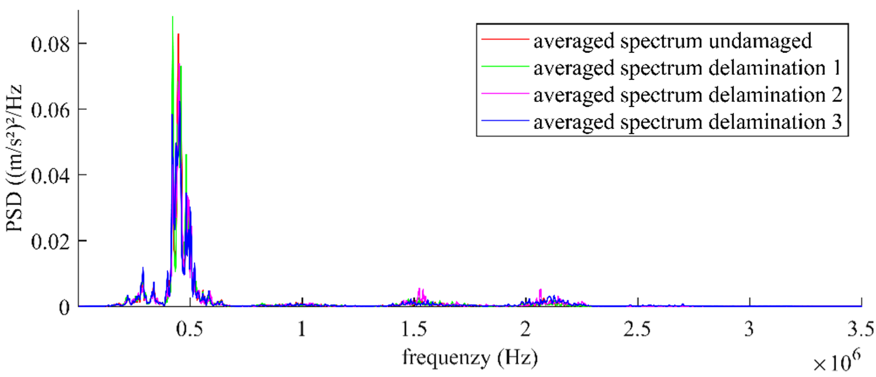

Fig. 6. Example of PSD: Averaged for each structural state.

A closer look at the spectra leads to the thesis that the main difference in the spectra are to be found between 1 MHz and 3,5 MHz, and again the changes for delamination two and three are much easier to identify. To test this the correlation coefficient of the spectra is computed in this area. The following figure shows the results for the correlation coefficient averaged for all received signals with excitation at T_6 (Fig. 7).

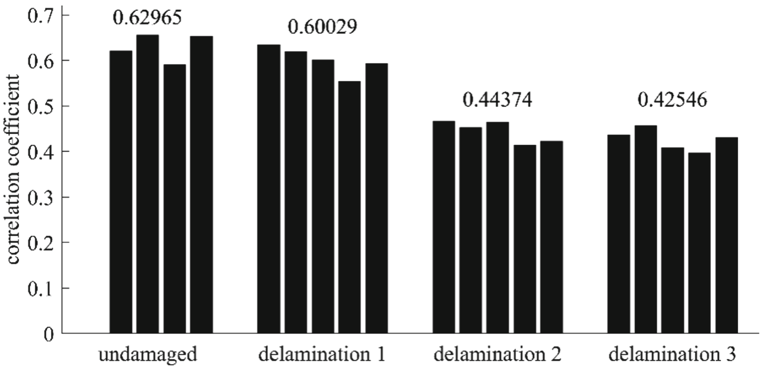

Fig. 7. Correlation coefficients: Comparing spectra averaged for each structural state.

A gap between measurement 9 and 10 can be identified not only in this example with excitation at T_6, but for all actuator-sensor combinations. This leads to the conclusion that mainly this change in the spectra of the signals is detected by the algorithms used in this paper.

Of course, other signal processing techniques have been used on the simulated data. Techniques known from classic guided waves SHM based on burst signals couldn't detect the damage due to the stochastic signals. The change in RMS- values also is not sufficient to detect delamination, even if it is calculated in the frequency range between 1 MHz and 3,5 MHz.

4 Conclusion and Outlook

The NSFD as well as the algorithm based on auto- and cross-correlation vectors are able to detect the structural changes in the simulated plate resulting from delamination at position two and three while position one is hardly visible. Further signal processing leads to the conclusion that small shifts in the power spectral density of the signals lead to the detection of the delamination. The simulations providing the necessary signals to test the algorithms run stable and are a powerful tool to optimize various features of the SHM-system: For example, number and position of the transducers or signal range of excitations signals. Furthermore, different kinds and positions of damage can be simulated in the future and the sensibility of damage detection algorithms can be tested. Of course, further investigation has to be done regarding the mentioned discrepancies between simulation and reality, namely by testing the algorithm with experimental data containing information about delamination. In addition, it needs to be tested if ongoing stochastic excitation shortens the lifetime of respective transducers. Another downside, as already mentioned, is the high sensitivity of the NSFD for changes in the environmental conditions (EOCs). Possibilities to differentiate between damage and changes in EOCs need to be found or clustering might be one possibility. A promising approach is the combination of different approaches to compensate the lack for EOC-compensation and damage localization.

Acknowledgments. The investigations took place within the framework of the R&D project KamoS and were kindly funded by the German Federal Ministry for Economic Affairs and Energy (project executing organization: German Aerospace Center, DLR) under the number 20Q1725D. Pawel Kudela would like to acknowledge the Polish National Agency for Academic Exchange for the support in the frame of the Bekker Programme (PPN/BEK/2018/1/00014/DEC/1). Jochen Moll acknowledges the supported by the Federal Ministry for Economic Affairs and Energy (grant no 03SX422B).

References

1. Moll, J., Kexel, C., Pötzsch, S., Rennoch, M., Herrmann, A.S.: Temperature affected guided wave propagation in a composite plate complementing the Open Guided Waves Platform. Sci. Data **6**(1), 1–9 (2019). https://www.nature.com/articles/s41597-019-0208-1.pdf
2. Brettschneider, J., Kraemer, P., Moll, J.: Alternative excitation and data analysis techniques for damage detection in metallic plates. In: The 12th International Workshop on Structural Health Monitoring, Stanford, California, USA, 10–12 September 2019. DEStech Publications, Inc., Lancaster, Electronic product, pp. 766–774 (2019)
3. Chang, Y., Yuan, F.-G.: Damage detection and localization via cross-correlation on metallic panels under ambient loading. In: The 12th International Workshop on Structural Health Monitoring, Stanford, California, USA, 10–12 September 2019. DEStech Publications, Inc., Lancaster, Electronic product, pp. 1975–1983 (2019)
4. Sabra, K.G., Srivastava, A., Lanza di Scalea, F., Bartoli, I., Rizzo, P., et al.: Structural health monitoring by extraction of coherent guided waves from diffuse fields. J. Acoust. Soc. Am. **123**(1) (2007). https://asa.scitation.org/doi/pdf/10.1121/1.2820800
5. Ostachowicz, W.M.: Guided waves in structures for SHM. The time-domain spectral element method. Wiley, Chichester, p. 337 (2012)
6. Kudela, P.: Parallel implementation of spectral element method for Lamb wave propagation modeling. Int. J. Numer. Methods Eng. **106**(6), 413–429 (2016). https://doi.org/10.1002/nme.5119
7. Kudel, P.: Vectorization of the code for guided wave propagation problems. In: EWSHM 2020, Palermo (2020)
8. Moll, J., Kathol, J., Fritzen, C.-P., Moix-Bonet, M., Rennoch, M., et al.: Open Guided Waves: online platform for ultrasonic guided wave measurements. Struct. Health Monit. **18**(5–6), 1903–1914 (2019). https://doi.org/10.1177/1475921718817169
9. Basseville, M., Abdelghani, M., Benveniste, A.: Subspace-based fault detection algorithms for vibration monitoring. Automatica **36** (2000)